

Part VI: Cyclic creep, nonlinearity and statistical scatter

The prediction formulas for the increase of creep due to superimposing a cyclic load upon a static load are derived and verified by six different data sets. Cyclic load effects upon both basic creep and drying creep are analyzed. The nonlinear dependence of uniaxial static (non-cyclic) creep upon stress is also quantified. The creep increase due to superimposed cyclic load is understood as the increase beyond the static creep that corresponds to the mean stress rather than the maximum stress. This appears to make the previously uncorrelated measurements of cyclic basic and drying creeps mutually consistent. It is found that load cycling accelerates only the basic creep but not the additional creep due to simultaneous drying. Since cyclic creep is necessarily a nonlinear phenomenon, a simple description of the nonlinear dependence of creep on stress is also given. Finally, the coefficients of variation of the deviations of formula predictions from the test data are evaluated (for all 80 data sets considered in this six-part study) and the average coefficients of variation to be expected in the predictions are indicated. They are overall much lower than those for the current formulations of CEB-FIP Model Code and ACI Committee 209.

INTRODUCTION

Pulsating loads, i. e., cyclic loads superimposed on a static load, represent a typical loading of many structures. They cause generally an increase of concrete creep compared to the prediction by the superposition principle. According to this principle, the mean creep strain caused by pulsating stress

$$\sigma = \sigma_0 + \frac{\Delta}{2} \sin(2\pi\omega t), \quad (52)$$

(where σ_0 = mean stress, $\Delta/2$ = cyclic stress amplitude, ω = frequency) would approach after many cycles the creep under static stress σ_0 . But in reality, a considerably higher value of mean strain is observed after many cycles, i. e., the pulsation of stress produces an additional inelastic strain, called cyclic creep.

A number of experimental studies ([78]-[83]) of cyclic creep have been carried out, but although many aspects have been clarified, a comprehensive practical model has not been developed. Especially, the differing observations of cyclic creep on sealed and drying specimens have not been mutually reconciled. The former ones indicate a cyclic creep that exceeds the static creep under the maximum stress $\sigma_{\max} = \sigma_0 + (\Delta/2)$, while the latter ones give a cyclic creep that is less, and so no clear trend with respect to σ_{\max} is indicated [84].

This discrepancy, however, is due to choosing as the basis for comparison the creep under the maximum stress σ_{\max} , while what one should really compare is the creep under σ_0 , the mean stress. This is because the comparison must be made with respect to the stress level which gives according to linear superposition an equivalent of the static creep. This is the level $\sigma = \sigma_0$ and not $\sigma = \sigma_{\max}$. It will be seen that if the comparison is made with regard to σ_0 , as used for sealed and unsealed specimens by Neville *et al.* ([78], [83]), then a pulsating load gives an increase of creep for both sealed and drying specimens, the increase for the drying ones being smaller. It will be shown, as one major result of this

study, that the difference in magnitude between sealed and unsealed specimens is explicable if one assumes that the superimposed cyclic load accelerates only the basic creep part of the total creep, and not the drying creep part.

Cyclic creep is essentially a nonlinear phenomenon, in terms of its stress dependence. Therefore, for the treatment of cyclic creep it is appropriate to include also the nonlinear dependence of static creep upon stress. This will be done according to the simple formulation from [4].

PROPOSED FORMULAS FOR CYCLIC BASIC CREEP AND NONLINEARITY

The following formula for ε/σ_0 , where ε represents the strain at the midpoints of cycles (i. e. at $\sigma = \sigma_0$), is proposed

$$J(t, t') = \left[\frac{1}{E_0} + C_{0c}(t, t') \right] f_{\sigma}, \quad (53)$$

where

$$C_{0c}(t, t') = \frac{\varphi_1}{E_0} (t'^{-m} + \alpha) (1 + k_{\omega} \varphi_{\sigma} \Delta^2 \omega^n) (t - t')^n, \quad (54)$$

which may be also written as

$$C_{0c}(t, t') = \frac{\varphi_1}{E_0} (t'^{-m} + \alpha) [(t - t')^n + k_{\omega} \varphi_{\sigma} \Delta^2 N^n], \quad (55)$$

where $N = (t - t')\omega$ = number of cycles. Parameters φ_1 , m , n , α and E_0 are the same as those defined in Part II [equations (15)-(19)]. Coefficient k_{ω} appears to be about 2.2 on the average and is mildly dependent on frequency ω or $N/(t - t')$. For $\omega \leq 680$ cycles/min., $k_{\omega} = 1.6$, and for $\omega \geq 1,500$ cycles/min., $k_{\omega} = 2.7$ if $f'_c \leq 3,000$ psi and $k_{\omega} = 2.4$ if $f'_c \geq 7,000$ psi, while between these values a linear variation may be assumed.

Functions f_σ and φ_σ define the nonlinearity of static and cyclic creep:

$$f_\sigma = \frac{R(\sigma_0)}{R(0.3)}, \quad \varphi_\sigma = \left[\frac{R(\sigma_{max})}{R(0.3)} \right]^{2.4} \quad (56)$$

$$R(\sigma) = 1 + 4.4 \left[1 - \sqrt{1 - (\sigma/f')^4} \right] \quad (57)$$

where f' = strength of the specimen at static loading.

Equations (54) and (55) reflect the fact that the time curves of cyclic creep at constant frequency appear to have the shape of power curves of the same exponent n as the static creep. This has been noted by Whaley and Neville [78]; however, their exponent was much too large ($n=1/3$) because they considered as creep only the deformation in excess of $1/E$ rather than that in excess of $1/E_0$. The similarity of time shapes and the identity of the exponents agrees with the hypothesis that the cyclic creep may be regarded as an accelerated creep. The dependence on the stress amplitude, $\Delta/2$, appears to be quadratic: Whaley and Neville [78] used a linear dependence on Δ along with $f_\sigma = \sigma_0 = 1$, but various exponents have been tried and exponent 2 worked best. In addition, a possible exponent on the bracketed expression $[(t-t')^n + k_\omega \varphi_\sigma \Delta^2 N^n]$ in equation (55) has been examined, but exponent 1 appeared to be no worse than other values.

Equation (55) is written in a form which is applicable even for irregular cycle shapes and periods, but constant amplitudes. There is no experimental confirmation of this, but the fact that the additional creep due to stress cycling is basically a non-viscoelastic phenomenon [equation (55)] and depends on the frequency only mildly, suggests this to be a reasonable assumption.

Function f_σ gives the nonlinear dependence of static basic creep upon stress σ_0 . The square-root type form in equation (57) is chosen for the purpose of giving a horizontal tangent at the peak stress point $\sigma=f'$; see reference [4]. Stress level $\sigma=0.3 f'$ is the typical level of long-time stresses in creep sensitive structures, and therefore the expressions for f_σ and φ_σ are introduced so as to give 1.0 at $\sigma=0.3 f'$.

The use of function φ_σ indicates that the additional cyclic creep depends nonlinearly not only on amplitude, $\Delta/2$, but also on the maximum stress, σ_{max} , and this effect is actually quite important already at medium stress levels. It indicates that cyclic creep can be high if σ_{max} is high, even though σ_0 may be low.

For experimental verification, only the test data of Whaley and Neville [78] (all obtained for $\omega=585$ cycles/min.) are sufficiently comprehensive. Their fits with the foregoing formulas are displayed as the solid lines in figure 39. The values $1/E_0$ and n have been both optimized, but the resulting value, $n=0.134$.

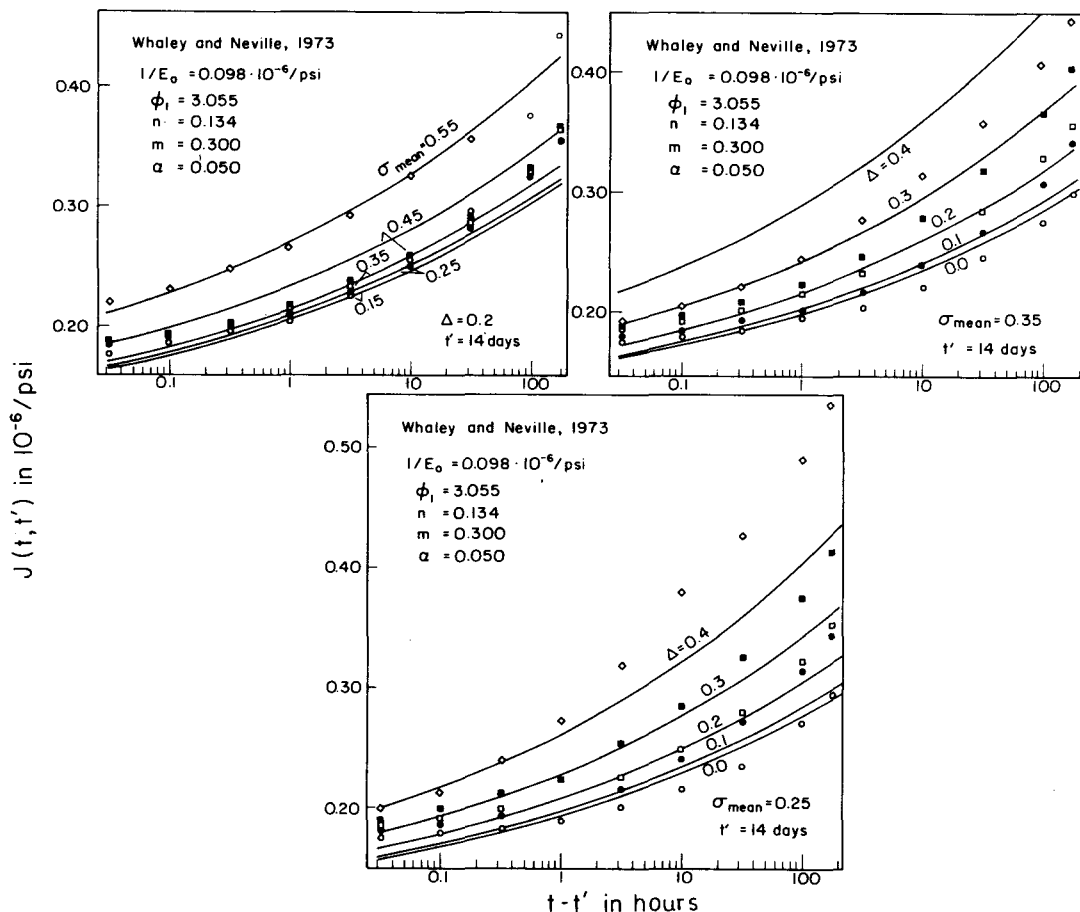


Fig. 39. — Fits of Cyclic Basic Creep Tests by Whaley and Neville (1973) [78].

came quite close to the value $n=0.145$ predicted by equations (17) and (18). These fits give a picture of the accuracy of the cyclic creep part of equation (54) when the error in predicting the basic creep is minimized. There is no check, anyway, on the value of $1/E_0$ because the initial elastic strain was not reported (see Appendix V). Because the unit creep strains reported were nearly the same for all σ_0/f' ratios up to 0.45 (at $\Delta=0.2$), the elastic strains were assumed to be the same (fig. 39).

PROPOSED FORMULAS FOR CYCLIC DRYING CREEP

The additional creep due to drying appears to be the same whether or not there is any cyclic stress component. Thus the strain ε/σ_0 where ε =strain at the midpoint of cycle ($\sigma=\sigma_0$) is:

$$J(t, t') = \left\{ \frac{1}{E_0} + C_c(t, t') + C_d(t, t', t_0) g_\sigma - C_p(t, t', t_0) \right\} f_\sigma \quad (58)$$

where $C_{cc}(t, t')$ and f_σ are given by equations (54)-(57). $C_d(t, t', t_0)$ is given by equation (26) (Part III).

$$C_p(t, t', t_0) = c_p k_h'' S_p(t, t_0) C_{cc}(t, t') \quad (59)$$

and

$$\left. \begin{aligned} g_\sigma &= \frac{R_d(\sigma_{\max})}{R_d(0.3f')} \\ R_d(\sigma_{\max}) &= 1 + 0.1 \left(\frac{\sigma_{\max}}{f'} \right)^2 \left[3 - \left(\frac{\sigma_{\max}}{f'} \right) \right] \end{aligned} \right\} \quad (60)$$

Functions $S_p(t, t_0)$, c_p , k_h'' are the same as given before [equations (28), (30), (29)].

The basic idea which led to the above formulas is that the additional creep due to drying does not get accelerated by cycling of the load. This is logical if the drying creep itself is regarded as an accelerated basic creep.

The decrease of creep that begins long after drying, $C_p(t, t', t_0)$ represents essentially an adjustment of the basic creep to a different humidity. Therefore the acceleration of creep due to load cycling should be applied to this term also. This is reflected by replacing $C_{cc}(t, t')$ from equation (27) of Part III by $C_{cc}(t, t')$, as indicated in equation (59). Function g_σ describes the fact that the drying creep term exhibits a stronger nonlinearity than the basic creep (see reference [4]). The expression for R_d is nearly the same as in reference [4], and is justified there.

To verify the foregoing prediction formulas for drying creep, five comprehensive data sets from the literature have been used ([79]-[83]). Fits of these data are exhibited in figure 40 by solid lines. For many data, the

strain at the midpoints of the cycles ($\sigma=\sigma_0$) was not indicated, rather, the strain peaks at σ_{\max} were reported. Therefore the values plotted in figure 40 are the values of $\varepsilon_{\max}/\sigma_0$, where ε_{\max} is the strain at the peak points ($\sigma=\sigma_{\max}$). This strain is predicted as

$$J(t, t')_{\max} = J(t, t') + \frac{\sigma_{\max} - \sigma_0}{E_{\text{dyn}} \sigma_0} f_\sigma \quad (61)$$

in which E_{dyn} is approximately assumed as the slope of the cyclic stress-strain diagram. Roughly, $1/E_{\text{dyn}} \approx J(t, t')/1.2$ for $t-t'=0.1$ day. In introducing equation (61) we adopt the view that ε_{\max} must properly be normalized with respect to σ_0 and not σ_{\max} as often used in the past, because the static linear creep under σ_{\max} is not equal to the theoretical cyclic creep according to the superposition principle (rather, it is the cyclic creep under mean stress, σ_0 , as already stated).

To obviate the error in the parameters for noncyclic creep and make the error due to the cyclic creep parameters alone more conspicuous, the parameters $1/E_0$ and $1/E_{\text{dyn}}$ [equation (61)], or $1/E_0$, $1/E_{\text{dyn}}$ and n , were optimized so as to achieve the best fit. The concrete mixture in references [79] and [80] was quite unusual ($w/c=0.9$, $f'_c=2,500$ psi, aggregate of max. size 6.4 mm), and in view of this fact the value of ϕ_d was also optimized independently for these data fits. Thus, the fits give an idea of accuracy in predicting cyclic drying creep when the static drying creep is known.

The test data used included various load frequencies ranging from 380 cycles/min. [81] to 3,000 cycles/min. [83], and these data provided the information on coefficient k_w as indicated after equation (55). The values of $J(t, t')$ at $N=20$ of Mehmehl and Kern's data were not included, since they appeared to be out of line (too high) and a much too big jump upwards was observed. Some other data of Gaede were too scattered, perhaps because of a lack of precise humidity control (55-70%), and these data were also omitted. Generally, Gaede's data cover comparatively short test periods ($t-t' \leq 4$ days). The initial elastic strain at σ_{\max} was not reported by Hirst and Neville [83] and so it had to be assumed (see Appendix V).

STATISTICAL SCATTER OF CREEP AND SHRINKAGE (FOR PARTS I-VI)

Having proposed in this six-part study the prediction formulas for creep and shrinkage, we should now indicate their accuracy. Some part of their error is no doubt systematic rather than random and could be eliminated by still more refined formulas. Lacking them, however, we have to treat the entire error as statistical in nature. The proper model, especially when an extrapolation of short-time measurements is needed, is a stochastic process [3], since it alone can correctly reflect the fact that an individual measured creep curve is usually quite smooth; for example, if the creep of one test specimen is high at a certain time, compared to the mean from

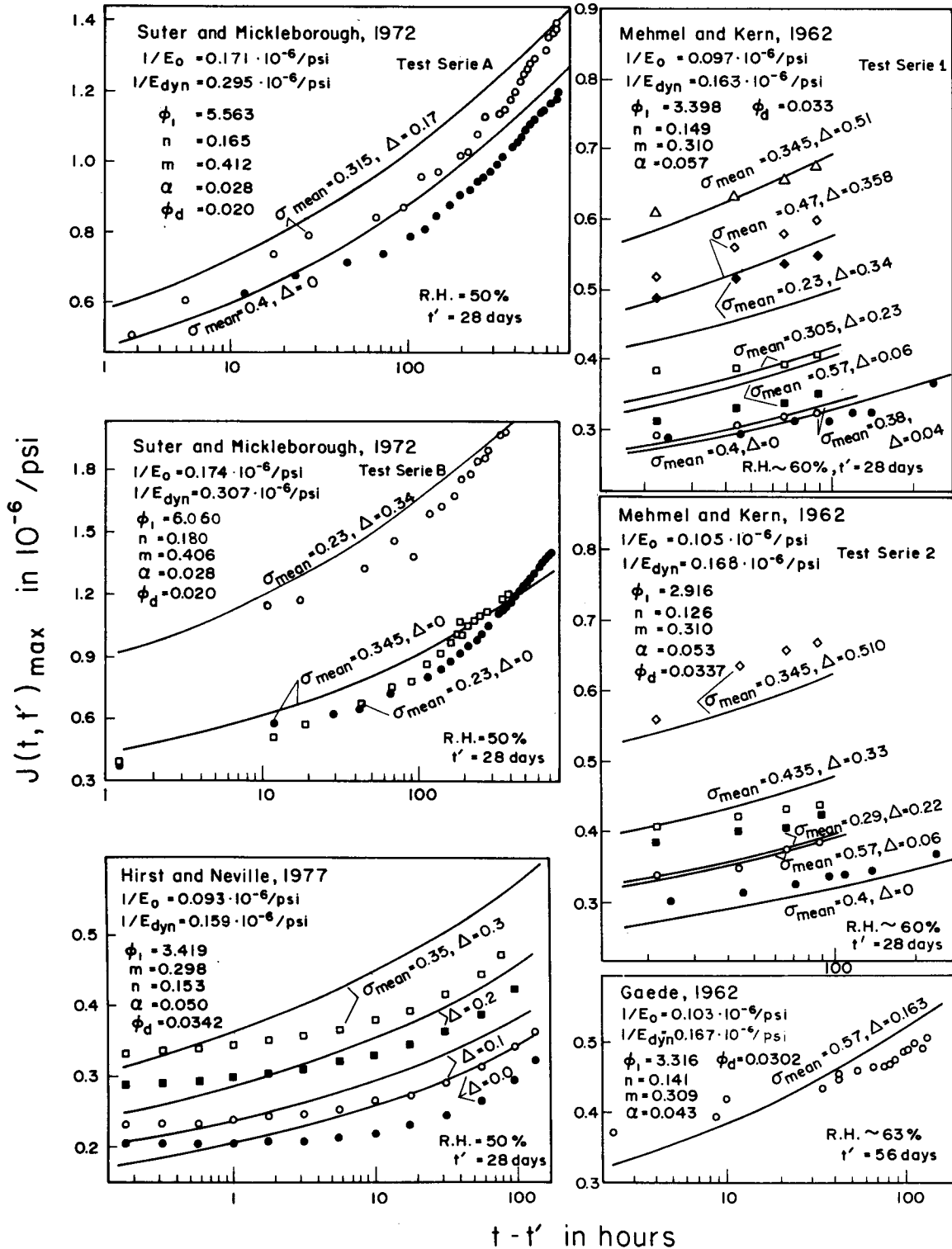


Fig. 40. — Fits of Cyclic Drying Creep Tests by Suter and Mickleborough (1972) ([79], [80]); Mehmel and Kern (1962) [81]; Hirst and Neville (1977) [83]; and Gaede (1962) [82].

many specimens, it will remain high for some time afterwards. Nevertheless, for the sake of simplicity, we will content ourselves with treating here the deviation from our formulas simply as a statistical variable.

In a detailed analysis, five different components of statistical scatter could be distinguished : a) measurement error; b) fluctuation in time due to the physical mechanism of creep and shrinkage; c) random effects of envi-

ronment and loading; d) random differences in properties of different specimens of the same concrete; and e) random differences between various concretes. There does not seem to exist, however, a sufficient data basis for this purpose. Nevertheless, it will be convenient to make a different distinction. We will consider the deviation of a measured point from our formulas to consist of two parts (see fig. 41):

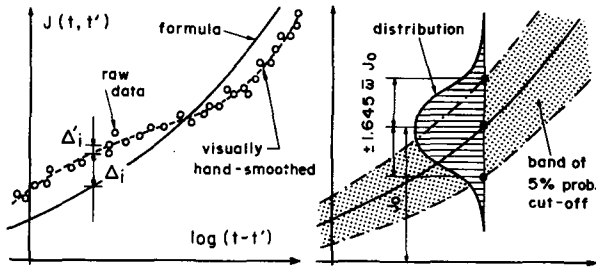


Fig. 41. — Statistical Scatter of Creep (or Shrinkage) Observations.

1. deviation Δ of a visually hand-smoothed experimental time curve [plotted versus $\log(t-t')$ or $\log(t-t_0)$] from our formulas:

2. deviation Δ' of a single measured point from the visually hand-smoothed experimental time curve.

The first part, Δ , is largely devoid of error type *a*) and partly of error *b*), and reflects mainly errors type *c*), *d*) and *e*) which are more important for structural design.

Within each data set j we calculate the unbiased estimate of the variance of our formula versus the visually hand-smoothed experimental curves:

$$s_j = \sqrt{\frac{1}{n-1} \sum_{i=1}^n \Delta_{ij}^2} \quad (62)$$

where $i=1, 2, \dots, n$ are the sampling points of data set j , which are chosen at constant spacing in $\log(t-t')$ or $\log(t-t_0)$ scale: the deviations of $J(t, t')$ or ϵ_{sh} from the hand-smoothed curve are calculated for each reported curve (e. g., $t'=\text{const.}$) shown in the preceding figures (Parts I-VI).

The values of s_j are not comparable from one concrete to another because a stronger concrete tends to have a smaller s_j just because of its strength. A parameter that is suitable for comparison is the coefficient of variation of data set j :

$$\omega_j = \frac{s_j}{J_j}, \quad \text{with } \bar{J}_j = \frac{1}{n} \sum_{i=1}^n J_{ij} \quad (63)$$

TABLE I

SUMMARY OF COEFFICIENTS OF VARIATION (IN PERCENT) FOR DEVIATION OF FORMULAS FROM TEST DATA (BASED ON TABLE II).

Type of data	E_0 or ϵ_{sh} optimized*		All by formulas	
	$\bar{\omega}$	$1.645\bar{\omega}$	$\bar{\omega}$	$1.645\bar{\omega}$
1. Shrinkage	13.3	21.9	31.7	52.1
2. Basic Creep	7.7	12.6	22.6	37.2
3. Drying Creep	11.9	19.6	16.6	27.3
4. Temp., Basic Creep	15.3	25.2	23.8	39.2
5. Temp., Drying Creep	14.5	23.8	24.7	40.6
6. Cyclic Basic Creep**	7.8	12.8	-	-
7. Cyclic Drying Creep	-	-	24.4	40.1
$\langle \omega \rangle = (\sum \bar{\omega}^2 / 6)^{1/2}$	12.1	19.9	24.4	40.0

*or E_0 from measured E_{28} , ** E_0 and n optimized

where J_{ij} are the values of visually hand-smoothed J -curve at sampling points $i=1, 2, \dots, n$, and \bar{J}_j is their mean. Putting now together all available data sets $j=1, 2, \dots, N$, we evaluate

$$\bar{\omega} = \sqrt{\frac{1}{N} \sum_{j=1}^N \omega_j^2} \quad (64)$$

which may be regarded as the overall variation coefficient relative to the mean value of creep. Note that $\bar{\omega}$ may be also expressed as

$$\bar{\omega} = \frac{1}{\bar{J}} \sqrt{\frac{1}{N(n-1)} \sum_{j=1}^N \sum_{i=1}^n (w_{ij} \Delta_{ij})^2}, \quad w_{ij} = \frac{\bar{J}}{J_j} \quad (65)$$

where \bar{J} = mean of \bar{J}_j . Thus $\bar{\omega}$ represents a weighted coefficient of variation, based on applying the weights \bar{J}/J_j to individual data sets. Analogous formulas have been used in evaluating shrinkage data. The values of $\bar{\omega}$ are tabulated in table I, and the values of $\bar{\omega}_j$ from which $\bar{\omega}$ values were obtained are tabulated in table II.

It is rather interesting to note that the coefficient of variation becomes greatly reduced if the elastic modulus is not predicted but is determined directly from experiment or if, in case of shrinkage, some shrinkage value is measured. For example, in case of basic creep, $\bar{\omega}$ drops from 23 to 8% (table II) if the elastic modulus is measured (or optimized). Finding better composition formulas for the elastic modulus would be the most effective way to improve the prediction of creep. But for drying creep (table II) this seems to be only partly so; curiously our formulas somehow predict the elastic modulus of drying concrete relatively better than that of sealed concrete.

A similar advantage can be gained if the concrete to be used resembles one for which test data are already available. A much smaller coefficient of variation of the prediction can then be expected.

Another noteworthy point (table II) is the fact that by deleting not more than one-third of the data sets used, substantially lower values of $\bar{\omega}$ would be obtained, and we would still have many data to support our formulation. Let us look, for example, at the data for shrinkage in table II. By deleting just 4 out of the 12 sets used, the coefficient of variation would drop from 31.7 to 12.6%! This shows that in making selective comparisons with test data one must be certain that the deleted data are either justifiably suspect or do not differ much from the data used.

The deviations Δ'_{ij} of actually measured points (raw data) from the visually hand-smoothed experimental creep or shrinkage curves normally yield the coefficient of variation $\omega' \approx 2\%$. To obtain the coefficient of variation ω for the deviation of the raw data from our formulas (fig. 41), we must superimpose ω' and $\bar{\omega}$. Assuming independent Gaussian distributions for Δ_{ij} and Δ'_{ij} , $\omega = (\bar{\omega}^2 + \omega'^2)^{1/2}$. Generally $\omega' \ll \bar{\omega}$, and then $\omega \approx \bar{\omega}$. If, e. g., $\bar{\omega} = 22\%$ and $\omega' = 2\%$, we get $\omega = 22.1\%$ and if $\bar{\omega} = 12\%$ and $\omega' = 2\%$, we get $\omega = 12.2\%$. Thus,

TABLE II

COEFFICIENTS OF VARIATION FOR DEVIATIONS OF FORMULAS FROM HAND-SMOOTHED DATA FOR INDIVIDUAL DATA SETS (IN PERCENT).

1. SHRINKAGE					
Set j	Ref. No.	ϵ_{sh} optimized		all by formulas	
		s_j	w_j	s_j	w_j
1	15	472	11.2	483	11.4
2	16	368	26.3	405	28.9
3	9	478	14.5	776	23.6
4	18	385	5.6	389	5.7
5	21	412	16.2	524	20.6
6	20a	675	12.4	757	13.9
7	20b	509	7.8	538	8.3
8	22	41	3.0	183	13.4
9	23	85	6.8	86	6.9
10	19c	375	18.6	416	20.6
11	19d	186	6.6	1830	62.7
12	17	258	8.5	2200	72.5
all			$\bar{\omega} = 13.3\%$		$\bar{\omega} = 31.7\%$

2. BASIC CREEP					
Set j	Ref. No.	E_0 optimized*		all by formulas	
		s_j	w_j	s_j	w_j
13	45	101	4.3	787	33.8
14	46-48	389	9.5	866	21.0
15	9,16	190	8.1	59	25.3
16	37,38e	783	8.0	1396	39.6
17	37,38f	704	15.6	1250	27.8
18	37,38g	283	8.5	553	16.6
19	36	118	3.8	1613	5.1
20	44	688	12.0	1257	22.0
21	23	79	3.7	347	16.1
22	25	188	3.1	362	5.9
23	20	205	3.3	1660	26.9
24	43h	143	4.1	552	15.9
25	43i	111	4.1	328	12.2
26	22	92	4.1	450	19.9
all			$\bar{\omega} = 7.65\%$		$\bar{\omega} = 22.6\%$

3. DRYING CREEP					
Set j	Ref. No.	E_0 optimized*		all by formulas	
		s_j	w_j	s_j	w_j
27	18	552	5.9	811	8.6
28	16j	410	10.4	1366	34.6
29	16k	784	15.9	182	3.7
30	36	199	5.3	227	6.1
31	19	153	3.6	276	6.5
32	25	1130	14.3	489	6.2
33	43	323	5.9	944	17.4
34	56k	126	2.7	420	9.0
35	56m	460	10.7	834	19.4
36	56n	179	3.2	309	5.5
37	56p	375	9.3	1088	27.1
38	56q	879	14.5	1299	21.5
39	56r	132	2.8	578	12.1
40	56f	74	1.6	74	1.6
41	56g	704	19.1	841	22.8
42	56t	984	24.8	556	14.0

LEGEND. s_j is in 10^{-7} for shrinkage, and in 10^{-10} per psi for creep ($\text{psi} = 6895 \text{ N/m}^2$); w_j is in percent; *or from measured E_{28} if available; $\dagger E_0$ and n optimized from basic creep data; a- size; b- age; c- w/c = 0.38; d- 0.55; e- Canyon Ferry Dam; f- Ross Dam; g- Shasta Dam; h- Mix A; i- Mix B; j- R.H. 50%; k- 1965; l- P2; m- P13; n- P23; o- P26-P29; p- P31; q- P32; r- P34-P35; s- P40-P41; t- P49; u- P50-P51; v- P52; w- P54; x- $t' = 100d$; y- $t' = 28d$; z- $t' = 28d$; G19; A- $t' = 90d$; G19; B- 270d; C- $t' = 28d$; G26; D- 90d; G26; E- 280d; G26; F- $\sigma_0 = 0.25 f'_c$; $\Delta = 0.1$ to 0.4 ; G- $\sigma_0 = 0.35 f'_c$; $\Delta = 0.1$ to 0.4 ; H- $\sigma_0 = 0.15$ to 0.25 ; $\Delta = 0.2$; I- Test Ser. 2; J- Test Ser. 1; K- Test A, L- Test B.

$\bar{\omega}$ is almost the same as ω , which validates our statistical method.

Creep-sensitive structures ought to be analyzed not only for the mean values but also the maximum and minimum values of creep and shrinkage, based on a certain specified probability cut-off. A 5% probability cut-off (i.e. a 95% confidence limit) is perhaps appropriate, and according to statistical tables it is given by relative deviations $\pm 1.645 \bar{\omega}$ (fig. 41), provided that Gaussian distribution is applicable. Such values (table I) should be used in the analysis of reactor vessels or containments, large span bridges or shells, tall buildings, ocean oil tanks, etc.

An interesting conceptual question is whether we should not calculate $\bar{\omega}$ assigning lower weights to certain test data sets that we suspect of being less reliable.

TABLE III

COMPARISON OF COEFFICIENTS OF VARIATION ω (IN PERCENT) FOR DEVIATIONS FROM TEST DATA, STRONGLY BIASED AGAINST LONGTIMES, LOW OR HIGH AGES AT LOADING, AND LARGE SIZE DRYING SPECIMENS (WHICH ARE CASES WHERE THE PRESENT MODEL CONTRIBUTES MOST).

Test Data	Present Model		Simplif. Model ³	ACI 1971	CEB 1978
	El.Mod. or ϵ_{sh} given ¹	All by eqs. ²			
1. Hansen, Mattock	11.2	11.4	13.4	33.6	72.7
2. L'Hermite ⁶ 1968 ⁴	19.3	22.7	35.2	82.1	35.0
3. L'Hermite ⁶ 1965	14.6	23.6	35.1	34.8	21.6
4. Troxell ⁷ et al.	5.6	5.7	11.3	55.5	84.5
5. Kesler ⁸ et al.	16.2	20.6	22.5	30.5	93.3
6. Keeton - size	12.4	13.9	12.1	52.1	80.7
7. Keeton - age	7.9	8.3	8.5	59.1	81.9
$\bar{\omega} = (\sum \omega_j^2/7)^{1/2}$	13.2	16.5	22.4	52.5	71.7
(95% conf. limit)**	(21.7)	(27.1)	(36.8)	(86.4)	(117.9)

2) BASIC CREEP					
8. L'Hermite ⁶ et al.	8.1	25.2	8.9	52.3	19.8
9. Canyon Ferry ³	8.0*	39.6*	45.4	47.3	18.7
10. Ross Dam ⁹	15.6*	27.7*	25.1	16.3	25.5
11. Shasta Dam ⁹	8.5	16.6	9.3	27.5	20.3
12. Dworshak Dam ¹⁰	12.0	21.2	12.5	30.0	45.4
13. Wylfa Vessel ¹¹	9.4	21.0	46.0	35.4	46.0
14. A. D. Ross	4.3	33.7	13.1	35.0	14.2
15. York et al. ¹³	3.6	16.1	9.0	23.2	8.7
16. Rostásy et al.	3.7	5.1	8.9	12.2	7.9
17. Keeton	3.3	26.9	49.2	36.4	52.4
18. McDonald	4.1	20.0	8.3	24.1	4.0
19. Maity, Meyers ¹⁴	4.1	14.2	30.5	15.4	27.5
$\bar{\omega} = (\sum \omega_j^2/12)^{1/2}$	8.0	24.0	27.2	31.9	28.6
(95% conf. limit)**	(13.2)	(39.5)	(44.7)	(52.5)	(47.0)

3) DRYING CREEP					
20. L'Hermite ⁶ , RH 50%	10.4	34.6	21.7	20.7	18.8
21. L'Hermite ⁶ 1965	15.9	3.7	8.0	25.6	9.8
22. Keeton	3.9	20.2	29.3	28.4	22.4
23. Troxell ⁷ et al.	5.9	8.6	4.4	31.3	27.5
24. Rostásy	5.3	6.1	17.1	8.0	16.9
25. Moossiosian ¹⁵	14.3	6.2	23.3	31.7	15.6
26. Maity, Meyers ¹⁴	5.9	17.4	14.7	35.3	27.0
27. Hummel et al.	36.2	6.5	12.8	10.3	16.3
28. Lambotte, Mommens ⁵	12.0	16.9	15.8	24.6	16.0
$\bar{\omega} = (\sum \omega_j^2/9)^{1/2}$	9.6	16.3	17.8	25.6	19.7
(95% conf. limit)**	(15.8)	(26.8)	(29.3)	(42.1)	(32.4)

4) COMBINED SHRINKAGE, BASIC CREEP AND DRYING CREEP					
$\langle \omega \rangle = (\sum \bar{\omega}_j^2/3)^{1/2}$	10.5	19.3	22.8	38.4	46.0
(95% conf. limit)**	(17.3)	(31.7)	(37.5)	(63.2)	(75.7)

LEGEND. ¹data for $t' = 2$ days included here but not for other columns, ²complete prediction, including elast. modulus, ³simplified version of the present model from Ref. 85, ⁴where hydration heat caused expansion zero strain was assumed, ⁵ $(\sum \omega_j^2/12)^{1/2}$ for 12 tests: P2, P13, P23, P26-29, P31, P32, P34-35, P40-41, P49, P50-51, P52 & P54, ⁶with Hamillan, ⁷with Raphael, Davis, ⁸with Wallo, Juan, ⁹Hanson, Harboe, ¹⁰Pirtz, ¹¹Browne et al., ¹²with Kennedy, Perry, ¹³mixes A and B, ¹⁴with Gamble, ¹⁵95% confidence limit in percent = 1.645 times the preceding line.

Perhaps the far-out data should be so treated, and we would then be pleased by getting much lower $\bar{\omega}$ values. However, to be certain of avoiding possible subjective bias, we prefer not to do that.

It is of interest to compare the present formulation to that of ACI Committee 209 (1971) [35 b] and of CEB-FIP Model Code 1978 [87]. A graphical comparison is carried out in reference [85] and the corresponding coefficients of variation are summarized in table III, which also includes the values for a simplified version of the present formulation that is presented in reference [85]. The last line compares the combined coefficient of variation, $\langle \omega \rangle$, for the entire model. The 95% confidence limits are given in parentheses.

Table III does not include all of the data sets used in table II because the intended scope of the ACI and

CEB Models is much narrower and it would be unjust to consider huge deviations for data for which these models are not intended (e. g., for ages at loading less than 7 days, temperature effect on shrinkage or creep, short-time shrinkage, etc.). The creep test data for various temperatures, both for basic and drying creep, as well as the cyclic creep data for basic and drying creep, are left out of the comparison because the ACI and CEB models either do not cover these cases or are so crude that the deviations are extremely large. It must be recognized, however, that the $\bar{\omega}$ values in table III for the present model would have been distinctly better had the present model been fitted exclusively to the data sets included in table III. This is one element of bias of table III in favor of ACI and CEB models.

The comparison in table III involves also another bias that strongly favors the ACI and CEB models compared to the present model. This is because the same weight has been given to all data sets, and within each set the same weight has been given to all sampling points ($i=1, 2, \dots$) uniformly spaced in log-time scale. Because the data points for medium ages at loading (around 28 days), for shorter creep durations (below 3 years), for small size drying specimens (3 to 6 inches) and for drying exposures at low ages are far more numerous, the comparison is strongly biased against small and high ages at loading, against long creep durations, against drying specimens of large sizes, and against specimens exposed to drying at higher ages. It is just in these cases where the present model makes the major improvement compared to the existing models (and some of these cases are actually most important for practice, e. g., creep of 40-year duration). The CEB and ACI models exhibit large errors in these cases but the data points are few and so the errors have little effect on the overall coefficient of variation.

The purpose of table III is to demonstrate that in spite of the bias which strongly favors the ACI and CEB models the present model is superior. For shrinkage the superiority is overwhelming. So it is for creep when the elastic modulus is known.

To remove the bias it would be necessary to first determine the number, n_{ik} , of the data sets that give information for each sampling location (i, k), i. e., for each combination of sampling age t'_k and sampling time $(t-t'_k)$, and then assign to each sampling point the weight $1/n_{ik}$. This would yield much larger weights on the relatively few data points that exist for small and high ages at loading and for long creep durations. Furthermore, one should also take into account the deviations in the final slope of the creep curves, which is important for extrapolation to a long service life. Such an unbiased comparison would be much more favorable to the present model (e. g., increasing the difference in $\bar{\omega}$ for the present and CEB models for basic creep to about 20%); but this approach has not been adopted in order to avoid any possible criticism that an uneven weight choice is subjective and that too much reliance is put on the few data sets that cover

extreme times. Table III is biased in one sense, while this would be biased in a different sense.

A totally unbiased choice of the method of comparison is impossible. It is for this reason that we have relied on a graphical display of the curves. For the ACI and CEB models, the curves are plotted in reference [85] against the same test data. A careful visual comparison with those plots is far more indicative, and it looks much more favorable to the present model than table III.

The fact that for creep the coefficients of variation of the CEB-FIP formulation are distinctly lower than those of the older ACI formulation is a result of a computer optimization of the fits of present data sets which was carried out at Northwestern University and led to a corrective initial deformation term (see reference [88]) that was proposed to be added to the expression from the preceding 1977 CEB final draft [39]. This proposed term has been subsequently adopted for the 1978 Model Code [87] under an equivalent but differently named and differently looking form (the so-called "irreversible deformation during the first few days", coefficient $\beta_a(t_0)$ in equation (e 6) on p. 333 of [87]; see reference [85]) and resulted in a substantial reduction of the deviations from available test data. This is another example of the usefulness of computer optimization.

CONCLUDING THOUGHTS

The scope of the comparisons with test data in this six-part study (80 different data sets) is unprecedented, and the degree of agreement distinctly surpasses the previous models. These results were made possible by a systematic use of the computer.

Perhaps the main advantage, compared to the existing model, is the fact that the temperature effect is modeled realistically. For many structures this is more important than usually thought.

Although the prediction formulas are simple enough, some engineers will no doubt be disappointed that they are not as simple as they would desire. For some strange reasons civil engineers are willing to perform very complicated structural calculations (stresses, deflections, failure, stability), but are unwilling to perform material property evaluations which are only half as complicated.

Nevertheless, let us hope that an even simpler but not cruder prediction model might be found in the future, and let us keep searching for it. In the meantime, though, we must recognize that with an electronic pocket calculator the evaluation of the present formulas is easy. Eventually, the code-preparing societies might consider a simplified version of the present model [85]. This would have to be weighed, though, against the inherent loss in the accuracy of prediction. The 95% confidence limits of the present model are already as high as about $\pm 40\%$ if no measurements are available.

Some engineers question whether an accurate prediction model is needed at all. They correctly point

out that much less was known about creep in the recent past, yet successful structures were built. They also contend that the statistical scatter of the behavior of concrete structures is so high that an accurate prediction model makes no sense. These advocates, however, serve nothing but impeding progress. We must not forget that the safety factors are getting lowered and more stringent demands for economy as well as safety, reliability and durability are inexorably being forced upon us engineers by the society. Among other things, we need more accurate prediction of creep and shrinkage to avoid the numerous cases of excessive deflections and damages due to cracking experienced in the past. Even more we need them to design accident-proof vessels for nuclear reactors, failproof oil storage tanks, record span bridges or shells and other special structures. At the same time we are finding that the statistical scatter of concrete properties is not that high if the influencing parameters are understood and controlled. And if we want to lower our safety factors and improve the long-term performance and reliability, we need, among other things, much more sophisticated models than those we have used so far.

APPENDIX VI

Basic Information on Data Used

Whaley and Neville's Tests on Cyclic Basic Creep (1973) [78]. — Specimens $76 \times 76 \times 203$ mm cast vertically, fog-cured at $20 \pm 1^\circ\text{C}$ for 14 days. During the test specimens were enclosed in polythene bags containing some water but not in direct contact with specimen. The relative humidity of the air surrounding the specimen was $\geq 98\%$, temperature $20 \pm 2^\circ\text{C}$. The cyclic load varied sinusoidally 585 cycles/min. Elastic strain for $\sigma_{\text{mean}} = 0.15$ to $0.45 f'$ assumed to be 0.170×10^{-6} /psi and 0.192 for $\sigma_{\text{mean}} = 0.55$. Water-cement-sand-gravel ratio 0.5 : 1 : 2 : 4. Quartzitic gravel aggregate, max. size 10 mm. Rapid hardening Portland cement. 14-day strength of prism ($76 \times 76 \times 203$ mm) 39 N/mm^2 .

Mehmel and Kern's Tests on Cyclic Drying Creep (1962) [8]. — Cylinders 150×600 mm, 1 day in mold then 6 days curing in water. At the age of 7 days specimens removed to test environment, 50-60% R.H. and temperature $20-21^\circ\text{C}$. R.H. in calculations assumed to be 60%. Specimens loaded at the age of 28 days. Frequency of sinusoidal loading 380 cycles/min. Cement Type I PZ 275. In test series 1 and 2 water-cement-sand-gravel ratios 0.44 : 1 : 1.51 : 3.01 and 0.47 : 1 : 2.7 : 4.81, cement contents 400 and 270 kg/m^3 . 28-day cube strength 488 and 483 kp/cm^2 correspondingly.

Suter and Mickleborough's Tests on Cyclic Drying Creep (1972) ([78], [90]). — Cylinders 76×30.5 mm, 1 day in mold, then cured in the tank until the 8th day and removed to the test room of 50% relative humidity and temperature 24°C . Cement Type III Canada HES 214 kg/m^3 . Water-cement-aggregate ratio 0.9 : 1 : 9.0. Max. size of aggregate 6.4 mm, and the fine aggregate followed the ASTM C 33 and CSA A 23.1 grading limits. Specimens loaded at the age of 28 days, frequency of sinusoidal cyclic load 1,500 cycles/min. The 28-day average cylinder (76×30.5 mm) strength in test series A and B = 2520 and 2580 psi correspondingly.

Gaede's Tests on Cyclic Drying Creep (1962) [82]. — Prisms ($100 \times 100 \times 500$ mm) 22 hours in mold, then in the water until the age of 7 days. Thereafter specimens in cellar at R.H. 55-70% and temperature $15-19^\circ\text{C}$. Relative humidity assumed to be 63%. Specimens loaded at the age of 56 days, frequency 665 cycles/min. Cement Type PZ 425, 354 kg/m^3 . Water-cement-sand-gravel ratio 0.585 : 1 : 1.986 : 3.107. 28-day cube strength 507 kp/cm^2 .

Hirst and Neville's Tests on Cyclic Drying Creep (1977) [83]. — Specimens prisms $76 \times 76 \times 203$ mm, fog cured at $20 \pm 1^\circ\text{C}$. Specimens loaded at the age of 28 days and allowed to dry at 50% R.H. The cyclic load sinusoidal, frequency 50 Hz (3,000 cycles/min.). Water-cement-sand-gravel ratio 0.5 : 1 : 2 : 4. Rapid hardening Portland cement was used. 28-day mean prism strength 46.5 N/mm^2 . Initial elastic strains at maximum stresses were not reported and were assumed to be 0.204, 0.225, 0.285 and 0.325×10^{-6} /psi at $\sigma_{\text{mean}} = 0.35 f'$ and $\Delta = 0, 0.1, 0.2$ and $0.3 f'$.

REFERENCES

- [78] WHALEY C. P., NEVILLE A. M. — *Non-elastic deformation of concrete under cyclic compression*. Magazine of Concrete Research, Vol. 25, No. 84, September 1973, pp. 145-154.
- [79] SUTER G. T., MICKLEBOROUGH N. C. — *Creep of concrete under cyclically varying dynamic loads*. Cement and Concrete Research, Vol. 5, No. 6, 1975, pp. 565-576.
- [80] MICKLEBOROUGH N. C. — *Creep of concrete under variable loading*. M. Eng. Thesis, Carleton University, Ottawa, 1972, 170 p.
- [81] MEHMEI A., KERN E. — *Elastische und plastische Stauchungen von Beton infolge Druckschwell- und Standbelastung*. Deutscher Ausschuss für Stahlbeton, Heft 153, Berlin 1962, Vertrieb durch Verlag von Wilhelm Ernst und Sohn.
- [82] GAEDE K. — *Über die Festigkeit und die Verformung von Beton bei Druck-Schwellbeanspruchung*. Deutscher Ausschuss für Stahlbeton, Heft 144, Berlin 1962, Vertrieb durch Verlag von Wilhelm Ernst und Sohn.
- [83] HIRST G. A., NEVILLE A. M. — *Activation energy of creep of concrete under short-term static and cyclic stresses*. Magazine of Concrete Research, Vol. 29, No. 98, March 1977, pp. 13-18.
- [84] BAŽANT Z. P. — *Langzeitige Durchbiegungen von Spannbetonbrücken infolge des Schwingkriechens unter Verkehrslasten*. Beton- und Stahlbetonbau, Vol. 63, December 1968, pp. 282-286.
- [85] BAŽANT Z. P., PANULA L. — *Simplified prediction of concrete creep and shrinkage from strength and mix*. Structural Engineering Report No. 78-10/640s, Northwestern University, Evanston, Illinois, October 1978.
- [86] BAŽANT Z. P., PANULA L. — *New model for practical prediction of creep and shrinkage*. Presented at A. Pauw Symp. on Creep, ACI Convention, Houston, October 1978, to be published.
- [87] CEB-FIP, *Model code for concrete structures*. Comité Euro-International du Béton, Paris, Vol. 2, April 1978, Appendix E.
- [88] BAŽANT Z. P., PANULA L. — *A note on amelioration of the creep function for improved Dischinger method*. Cement and Concrete Research, Vol. 8, No. 3, 1978, pp. 381-386.

RÉSUMÉ

Un modèle de prévision pratique des déformations du béton en fonction du temps.

V. Influence de la température sur le fluage en séchage. — On applique ici à l'influence de la température le modèle de fluage décrit dans la troisième partie. On conserve la forme de base qui est celle d'une forme additive de la loi de double puissance et du terme qui correspondrait au fluage, mais certains coefficients deviennent dépendants de la température afin de traduire l'accélération du séchage et du vieillissement. On obtient une bonne concordance avec les résultats d'essai.

VI. Fluage cyclique, non-linéarité et dispersion statistique des résultats. — Les formules de prévision de l'accroissement de fluage dû à la superposition d'une charge cyclique à une charge statique que l'on a obtenue ont été vérifiées par six séries différentes de données. On a étudié sous charge cyclique les accroissements tant du fluage de base que du fluage de séchage. On a quantifié

la relation non linéaire à la contrainte du fluage uniaxial sous chargement statique. Ce que l'on entend ici par accroissement du fluage est l'accroissement au-delà du fluage statique qui correspond à la contrainte moyenne plutôt qu'à la contrainte maximale. Il semble que c'est ce qui détermine la consistance entre les mesures du fluage de base cyclique et du fluage de séchage que l'on n'avait pas jusque-là reliées, et on établit que l'allure cyclique de la charge accélère uniquement le fluage de base mais non le fluage additionnel dû au séchage simultané. Étant donné que le fluage cyclique est nécessairement non linéaire, on présente aussi une description simple de la relation non linéaire du fluage à la contrainte. Enfin, on indique les coefficients de variation des formules tirées des résultats d'essai (pour les 80 résultats examinés dans les 6 parties de cette étude) et les coefficients moyens de variation prédictibles. Ils sont dans l'ensemble assez inférieurs à ceux que l'on trouve dans les formules courantes du Code Modèle CEB-FIP et de la Commission 209 de l'ACI.